

Feature Space Topology Control via Hopkins Loss

Einari Vaaras

Signal Processing Research Centre
Tampere University
Tampere, Finland
einari.vaaras@tuni.fi

Manu Airaksinen

BABA Center, Department of Physiology
University of Helsinki
Helsinki, Finland
manu.airaksinen@helsinki.fi

Abstract—Feature space topology refers to the organization of samples within the feature space. Modifying this topology can be beneficial in machine learning applications, including dimensionality reduction, generative modeling, transfer learning, and robustness to adversarial attacks. This paper introduces a novel loss function, Hopkins loss, which leverages the Hopkins statistic to enforce a desired feature space topology, which is in contrast to existing topology-related methods that aim to preserve input feature topology. We evaluate the effectiveness of Hopkins loss on speech, text, and image data in two scenarios: classification and dimensionality reduction using nonlinear bottleneck autoencoders. Our experiments show that integrating Hopkins loss into classification or dimensionality reduction has only a small impact on classification performance while providing the benefit of modifying feature topology. The code is freely available at https://github.com/SPEECHCOG/hopkins_loss.

Index Terms—Hopkins statistic, feature shaping, feature space topology, autoencoders, dimensionality reduction.

I. INTRODUCTION

The concept of *feature space topology* refers to how samples are organized in the feature space. In the context of machine learning (ML), modifying features into a desired topology can be potentially useful in multiple contexts: First, imposing a specific structure on the feature space during ML model training might improve generalization. For example, regularly-spaced features might help in reducing overfitting by ensuring that the features are uniformly distributed [1, 2]. Second, when using nonlinear bottleneck autoencoders (AEs), transforming high-dimensional data into a lower-dimensional feature space with a desired feature topology may be beneficial for e.g. visualization, data compression, or as a pre-processing step for other ML algorithms such as for classification purposes [3–6].

Third, controlling the distribution of generated features in generative models, such as generative adversarial networks [7], may be useful in applications such as image synthesis, where the spatial arrangement of features is important [8–10]. Fourth, constructing features with specific topological properties may benefit domains like bioinformatics, where the spatial arrangement of features (e.g. genes) can be critical [11, 12]. Fifth, in transfer learning, adjusting the feature space topology of the source or target domain can help in aligning the respective feature spaces [13–16]. Finally, controlling feature space topology might make ML models more robust to adversarial attacks, as the topology of the feature space may affect the sensitivity of ML models to perturbations [17–19].

In this paper, we propose a novel loss function called Hopkins loss, which is based on the Hopkins statistic (H , see Section II-A). This loss function can be integrated into ML model training to modify or enforce the feature space into either a regularly-spaced, randomly-spaced, or clustered topology. This is in contrast to existing topology-related methods (Section II-B) that all aim to preserve the topology of input features rather than try to transform it into a user-defined form. We evaluate the effect of Hopkins loss on speech, text, and image data in two scenarios: classification and dimensionality reduction using AEs.

The paper is organized as follows. First, Section II gives an overview of literature relevant to the present study, namely H (Section II-A) and ML methods related to feature space topology (Section II-B). Then, Hopkins loss is detailed in Section III, after which experimental details are given in Section IV. Finally, results are presented in Section V, and conclusions are drawn in Section VI.

II. RELATED WORK

A. Hopkins statistic

H is a statistical hypothesis test measuring the clustering tendency of a dataset [20]. In H , the null hypothesis is that the data is generated by a Poisson point process (uniformly randomly distributed), while the alternative hypothesis is that the data points are clustered [20, 21]. Values of H are in the range $[0, 1]$, where values greater than 0.75 indicate a clustering tendency at a 90% confidence level [21]. Hopkins and Skellam [20] introduced H to study the 2D spatial distribution (i.e. coordinates) of trees within a given area. Cross and Jain [22] studied the use of H as a pre-processing step before subjecting data to a clustering algorithm, experimenting with low-dimensional real and simulated datasets. Lawson and Jurs [21] extended H for both artificial and real chemical datasets. Banerjee and Davé [23] used H to validate the presence of meaningful clusters in data using simulated 2D datasets.

H has also been used in more recent studies. In a study by Li et al. [24], the authors developed a method to enhance indoor localization accuracy by identifying direct and indirect signal conditions using H . They used H to measure the spatial randomness of the received signal strength data. Zhang et al. [25] proposed a novel density peaks clustering algorithm that integrates H to address the limitations of other similar clustering algorithms related to density measurement and cluster

center identification. In their study, H was used to determine whether the data points were randomly distributed or clustered in order to identify potential cluster centers.

B. Machine learning related to feature space topology

The concept of feature space topology has appeared in ML literature multiple times. Hu et al. [2] proposed a loss function for image segmentation that aims to preserve the feature topology of the reference segmentation, demonstrating effectiveness across various natural and biomedical datasets. Brüel-Gabrielsson et al. [17] introduced a differentiable topology layer that uses persistent homology to first analyze the input data at multiple scales, and then preserve its topology. They demonstrated the usefulness of their method for tasks where the shape and structure of the data are important, such as incorporating topological priors in generative models. The topological loss function presented by Malyugina et al. [26] is also based on persistent homology, and it was designed for image denoising in low-light conditions. They combined their loss function with L1 and L2 losses to ensure that the denoised image maintains the same topology as the original noisy image, and they showed that their approach helped to reduce artifacts and preserve important structural elements of the input image.

Alberti et al. [27] proposed a method for representing manifolds of arbitrary topology using a mixture model of variational AEs. Their method learns the manifold’s topology from the data and solves inverse problems by minimizing a data fidelity term restricted to the manifold, demonstrating effectiveness in applications such as deblurring and electrical impedance tomography. Mi et al. [28] proposed an adversarial training approach based on a topology-preserving regularization term that maintains neighborhood relationships in the representation space, demonstrating enhanced classification accuracy on multiple image datasets.

III. HOPKINS LOSS

H is computed as follows [21, 23]:

- 1) Let X be a set of n d -dimensional data points.
- 2) Select a random sample of $m \ll n$ data points sampled from X without replacement, denoted as \tilde{X} .
- 3) Generate a set Y of m data points uniformly distributed at random.
- 4) Define two distance measures, both computed using distance metric D :
 - a) u_i : The minimum distance of $y_i \in Y$ from its nearest neighbor in X .
 - b) w_i : The minimum distance of $\tilde{x}_i \in \tilde{X}$ from its nearest neighbor in X .

$$5) \text{ Calculate the statistic as: } H = \frac{\sum_{i=1}^m u_i}{\sum_{i=1}^m u_i + \sum_{i=1}^m w_i} \quad (1)$$

The computation of H leads to values of $H \approx 0.5$ for randomly-spaced data, $H \in [0.01, 0.3]$ for regularly-spaced data, and $H \in [0.7, 0.99]$ for clustered data [23]. Figure 1 shows

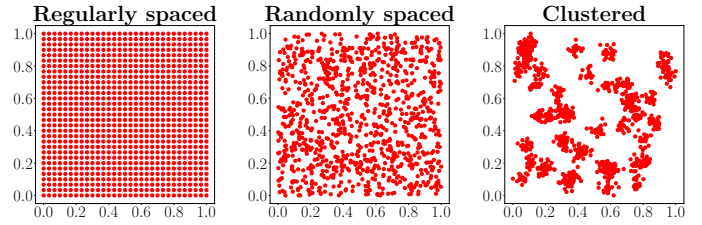


Fig. 1. An example 2D visualization of regularly-spaced (left, $H \in [0.01, 0.3]$), randomly-spaced (middle, $H \approx 0.5$), and clustered data (right, $H \in [0.7, 0.99]$) using the distance metric $D = \text{Chebyshev}$.

examples of data with different values of H . In our preliminary experiments using simulated data with different feature topologies, $n \in [1k, 100k]$, and $d \in [2, 512]$, out of the tested $D \in \{\text{Euclidean, Manhattan, cosine, Mahalanobis, Chebyshev}\}$ only Chebyshev distance was able to maintain the desired¹ properties of H across all tested conditions. Consequently, $D = \text{Chebyshev}$ in the present study.

By calculating H using differentiable operations, H can be integrated into a loss function. Consequently, we define the Hopkins loss, L_H , as

$$L_H = |H - H_T|, \quad (2)$$

where H_T is a pre-defined target value for H . Minimizing L_H causes the neural network-based model to transform the feature topology of the input features towards the topology defined by H_T . For example, with $H_T = 0.01$, minimizing L_H leads to the model to learn regularly-spaced features.

In our preliminary experiments, we observed that generating the randomly-distributed set Y within the feature space of the minibatch samples (i.e., set X) led to better and more consistent results. Therefore, the values in Y are scaled and shifted using the minimum and maximum values of X before computing u_i in order to better align with the feature space of X . Furthermore, Ripley [29] suggested that $m < 0.1n$, and Dubes and Jain [30] suggested using $m = 0.05n$ to ensure that nearest-neighbor distances are independent, thereby approximating a Beta distribution. We did not find any difference in $m = kn$ between $k \in \{0.02, 0.05, 0.08\}$ in our preliminary experiments, which led to the selection of $m = 0.05n$ for the present experiments, following Dubes and Jain [30].

IV. EXPERIMENTS

We experimented with L_H using speech, text, and image data (Section IV-A) in both classification (Section IV-B) and dimensionality reduction using AEs (Section IV-C). The aim was to determine whether the use of L_H improves, degrades, or does not affect classification performance, and to assess the impact of L_H on feature topology (in terms of H). We implemented the code using PyTorch version 1.13.1, and we used an NVIDIA Tesla V100 GPU to train our models. Our implementation is publicly available on GitHub.²

¹ $H \in [0.01, 0.3]$ for regularly-spaced data etc.

²https://github.com/SPEECHCOG/hopkins_loss

A. Data

The Ryerson Audio-Visual Database of Emotional Speech and Song (RAVDESS) [31] is a multimodal dataset comprising 7,356 recordings performed by 24 professional actors. For the purposes of this study, we utilized 1,440 speech-only recordings from RAVDESS, including eight distinct emotional categories. For each recording, eGeMAPS [32] feature vectors with a dimensionality of $d = 88$ were extracted using the openSMILE toolkit [33], and the feature vectors were z-score normalized at the dataset level. We randomly split the speaker-wise data into training, validation, and test sets in a 60:20:20 ratio, ensuring that no speaker’s data appeared in more than one set.

The IMDB movie review dataset [34] is designed for binary text sentiment classification, containing an even number of positive and negative movie reviews for a total of 50,000 highly polar reviews (25,000 for training and 25,000 for testing). The pre-trained BERT [35] tokenizer and model were used from the Hugging Face Transformers library [36] to first tokenize the text data, and then to convert the CLS tokens into outputs of dimensionality $d = 768$. We randomly split the 25,000 training reviews into training and validation sets in an 80:20 ratio.

The Fashion-MNIST dataset [37] consists of 70,000 grayscale images of 10 distinct fashion products, with 7,000 images per category and each image sized 28x28 pixels. The dataset includes 60,000 training images and 10,000 testing images, and it was normalized at dataset-level to have pixel values in the range $[-1.0, 1.0]$. Each image was flattened to obtain feature vectors of dimensionality $d = 784$. The 60,000 training images were randomly split into 50,000 training and 10,000 validation samples.

B. Classification experiments

We trained simple multi-layer perceptron (MLP) networks for speech emotion recognition (SER) on RAVDESS, text sentiment classification (TSC) on the IMDB movie review dataset, and image classification (IC) on Fashion-MNIST. The MLP network consisted of two fully-connected Gaussian error linear unit (GELU) [38] layers followed by a linear layer and a softmax function. The GELU layers were followed by a dropout of 20%. The model output dimensionalities were 128, 128, and C , where $C \in \{2, 8, 10\}$ represents the number of classes for text, speech, and image data, respectively.

For model training, we used a combination of two loss functions, categorical cross-entropy loss, L_{CE} , and L_H :

$$L = w_C L_{CE} + (1 - w_C) L_H . \quad (3)$$

Here, $w_C \in [0, 1]$ is the weight for the classification loss L_{CE} . For example, with $w_C = 1$, L_H is not utilized during model training, whereas with $w_C = 0.5$ the terms L_{CE} and L_H in Equation 3 are given equal weight during model training. Based on preliminary experiments, we found it most effective to compute L_H from the output of the second MLP layer, and to use $w_C = 0.75$ when both L_{CE} and L_H were used simultaneously.

We used a minibatch size of 1024 samples and an initial learning rate of 10^{-4} with a reduction factor of 0.5 based on

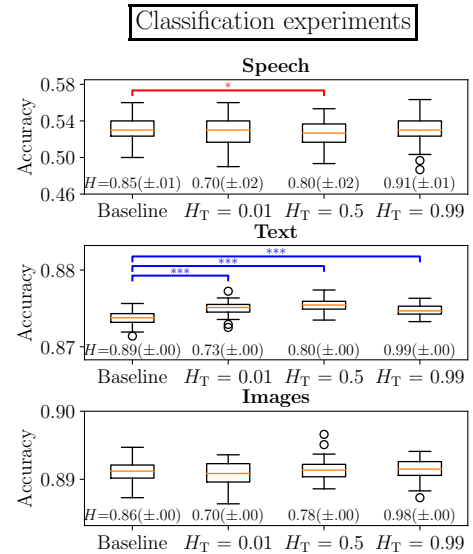


Fig. 2. The results of the classification experiments. The Hopkins loss target values $H_T = 0.01$, $H_T = 0.5$, and $H_T = 0.99$ aim at learning regularly-spaced, randomly-spaced, and clustered features, respectively. Statistically significant differences are reported using the Mann-Whitney U test [40] with either * ($p < 0.05$), ** ($p < 0.01$), or *** ($p < 0.001$). Results significantly higher than the baseline are marked with blue, and vice versa with red. The number below each box plot is the mean H value ($\pm 95\%$ confidence interval).

the validation loss with a patience of 30 epochs. Adam [39] optimizer and early stopping with a patience of 100 epochs based on the validation loss were used, and the model with the lowest validation loss was then used for testing model performance on the test set. Since the class categories in all three datasets of the present experiments had balanced class distributions, accuracy was used as the performance metric on all three tasks. Using all three datasets, we tested all possible combinations of $H_T \in \{0.01, 0.5, 0.99\}$ and $w_C = 0.75$. As a baseline, we used $w_C = 1.0$. Each experiment was repeated 100 times to account for variability in random model initialization.

C. Autoencoder experiments

We trained AEs to first compress the input features’ dimensionality for each of the three datasets, after which we extracted bottleneck features of the entire dataset using the trained AE. Then, to assess feature degradation, we tested the classification performance of the bottleneck features using a linear classifier for SER on RAVDESS, TSC on the IMDB movie review dataset, and IC on Fashion-MNIST. The AE consisted of an encoder and a decoder, and the encoder was an MLP network consisting of two fully-connected GELU layers followed by a linear layer, and the first two layers were followed by a 20% dropout. The encoder output dimensionalities were 128, 128, and B , where $B \in \{32, 8, 2\}$ stands for the bottleneck feature dimensionality. The decoder was simply a mirrored version of the encoder.

For AE training, we used a combination of two loss functions, L_H and mean squared error loss, L_{MSE} , in the following manner:

$$L = w_R L_{MSE} + (1 - w_R) L_H . \quad (4)$$

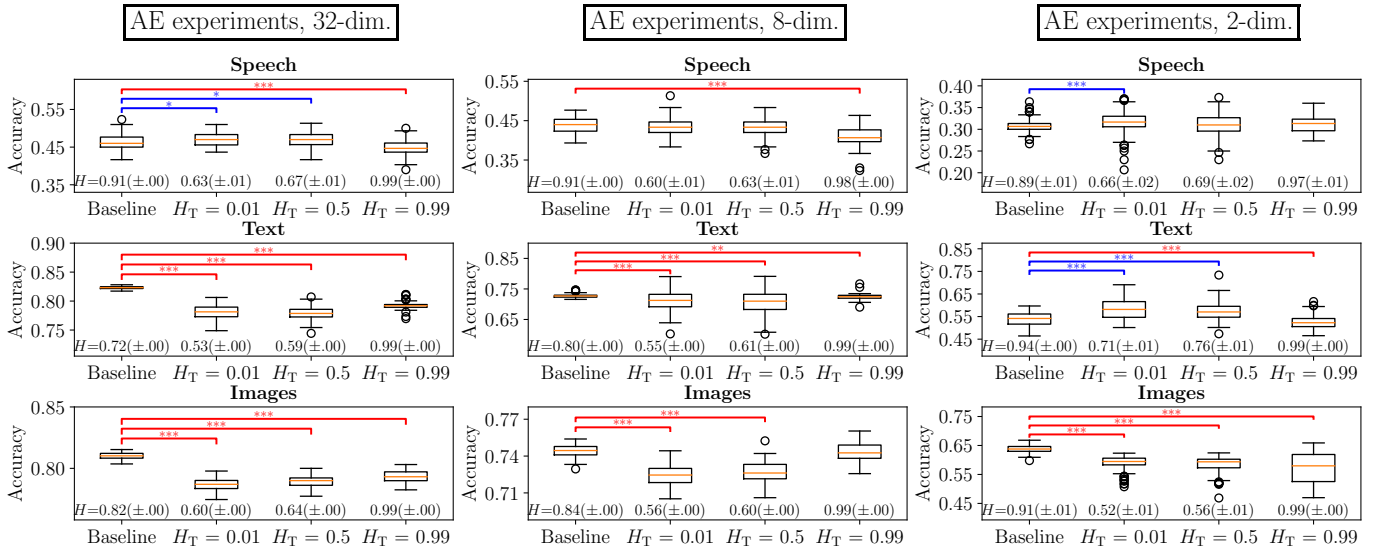


Fig. 3. The results of the AE experiments (left: bottleneck feature dimensionality $B = 32$, middle: $B = 8$, right: $B = 2$). The Hopkins loss target values $H_T = 0.01$, $H_T = 0.5$, and $H_T = 0.99$ aim at learning regularly-spaced, randomly-spaced, and clustered features, respectively. Statistically significant differences are reported using the Mann-Whitney U test [40] with either * ($p < 0.05$), ** ($p < 0.01$), or *** ($p < 0.001$). Results significantly higher than the baseline are marked with blue, and vice versa with red. The number below each box plot is the mean H value ($\pm 95\%$ confidence interval).

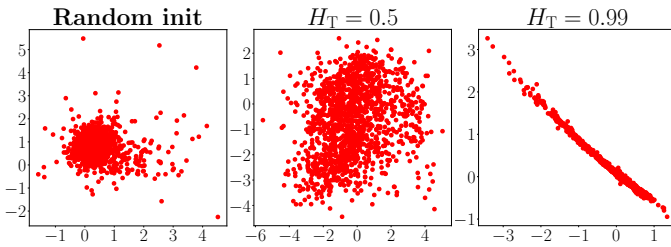


Fig. 4. Example of a 0.10 difference in H value when bottleneck feature dimensionality $B = 2$ for the RAVDESS dataset. The bottleneck features of a randomly initialized model (left, $H = 0.89$), a trained model with L_H and $H_T = 0.5$ (middle, $H = 0.79$), and a trained model with L_H and $H_T = 0.99$ (right, $H = 0.99$) are shown.

Here, $w_R \in [0, 1]$ is the weight for the reconstruction loss L_{MSE} . Based on preliminary experiments, we compute L_H from the output of the bottleneck layer of the encoder, and use $w_R = 0.75$ when both L_{MSE} and L_H were used simultaneously.

After extracting the bottleneck features using the trained AE, an MLP classifier consisting of a single linear layer and a softmax function was trained for classification using the bottleneck features as the model input. For both the AE and classifier training, we used the same hyperparameters and training pipeline as described in Section IV-B with the only exceptions of having $4 \cdot 10^{-4}$ as the initial learning rate for both AE and classifier training, and without including L_H in classifier training. We tested all possible combinations of $H_T \in \{0.01, 0.5, 0.99\}$, $B \in \{32, 8, 2\}$, and $w_R = 0.75$. As a baseline, we tested all combinations of $B \in \{32, 8, 2\}$ and $w_R = 1.0$. Each experiment was repeated 100 times to account for the minor variability caused by the random initialization of model weights.

V. RESULTS

Figure 2 presents the classification experiment results (Section IV-B). For speech and image data, integrating L_H into model training generally does not degrade model performance, while also adding the benefit of modifying the features towards a desired topology. Additionally, for text data, adding L_H outperformed the baseline for all targeted feature topologies. On average, including L_H in the classification experiments modified H towards the target value H_T by approx. 0.09, 0.11, and 0.12 in terms of H value for speech, text, and image data, respectively.

Figure 3 shows the AE experiment results (Section IV-C). In most cases, the use of L_H resulted in lower classification performance compared to the baseline, which is natural since L_H was not part of the classifier training in AE experiments. However, there were multiple cases where the use of L_H resulted in either a similar or even higher classification performance than the baseline. In AE experiments, the modification in feature space topology was notably larger than in the classification experiments: On average, the inclusion of L_H in the AE training modified H towards the target value H_T by approx. 0.19, 0.18, and 0.22 in terms of H value for speech, text, and image data, respectively. As a reference, Figure 4 illustrates a 0.10 difference in terms of H value in 2D space when using L_H with AEs. Note that since the samples are already organized into a single large cluster for the randomly-initialized model, with L_H and $H_T = 0.99$ it is easier to optimize forming one large cluster than multiple clusters during model training. Overall, the average decrease in performance in the AE experiments is relatively small compared to the average change in H values.

Interestingly, for both classification (Figure 2) and AE (Figure 3) experiments, the feature topologies for all baseline

TABLE I

COMPARISON OF TRAINING EPOCH DURATIONS WITH THE USE OF L_H AND WITHOUT IT (BASELINE) ACROSS CLASSIFICATION AND AE EXPERIMENTS.

NO NOTABLE DIFFERENCES IN EPOCH DURATIONS WERE OBSERVED ACROSS DIFFERENT H_T VALUES, AND THEREFORE BOTH THE MEAN AND STANDARD DEVIATION (SD) OF EPOCH DURATIONS ARE COMPUTED ACROSS ALL TRAINING EPOCHS AND H_T CONFIGURATIONS. FOR EACH EXPERIMENTAL CONDITION, THE AVERAGE COMPUTATIONAL OVERHEAD OF USING L_H ACROSS ALL THREE DATASETS IS HIGHLIGHTED IN RED TEXT.

	Speech	Text	Images	L_H , avg. Δ
Classification, baseline	0.01 (\pm .00)	0.22 (\pm .02)	0.77 (\pm .05)	
Classification, L_H	0.01 (\pm .01)	0.26 (\pm .03)	0.87 (\pm .08)	+10%
AE (32-dim.), baseline	0.01 (\pm .00)	0.22 (\pm .02)	0.77 (\pm .08)	
AE (32-dim.), L_H	0.01 (\pm .01)	0.28 (\pm .02)	0.83 (\pm .08)	+12%
AE (8-dim.), baseline	0.01 (\pm .00)	0.23 (\pm .03)	0.77 (\pm .07)	
AE (8-dim.), L_H	0.01 (\pm .01)	0.28 (\pm .03)	0.88 (\pm .07)	+12%
AE (2-dim.), baseline	0.01 (\pm .00)	0.25 (\pm .03)	0.75 (\pm .06)	
AE (2-dim.), L_H	0.01 (\pm .01)	0.29 (\pm .03)	0.92 (\pm .07)	+13%

Avg. epoch duration (s) (\pm SD)

models were clustered in terms of H value, indicating a natural bias towards a clustered topology in the original features. This may explain why L_H could not force the features into a regularly-spaced topology ($H \in [0.01, 0.3]$) with $H_T = 0.01$. Another potential explanation for why L_H could not enforce a regularly-spaced topology is that this may be inherently a more difficult task for the model: structuring features uniformly might require more effort than modifying them to be randomly spaced or clustered. However, the experiments showed that L_H can be used to adjust the original clustered topology towards being more regularly spaced.

Table I compares the duration of training epochs with and without the use of L_H . Overall, the computational overhead introduced by L_H is modest, with an average increase in epoch duration across all three datasets of approximately 10–13% in all experimental conditions. For the smallest dataset, RAVDESS, the overhead was marginal. In contrast, the two other datasets, each notably larger than RAVDESS in terms of sample count and feature dimensionality, exhibited a more noticeable increase in training time when L_H was applied. These results suggest that the computational cost of L_H scales with both dataset size and feature dimensionality. Furthermore, in several cases, the use of L_H led to a slight increase in the variability of epoch durations, as reflected by a higher standard deviation. However, it is important to note that these results may vary depending on factors such as model complexity, dataset characteristics, and the hardware used for training.

VI. DISCUSSION AND CONCLUSION

This paper presented a novel loss function, L_H , to modify features into a desired topology. We evaluated L_H on speech, text, and image data in two scenarios: classification and dimensionality reduction using AEs. As a result, integrating L_H into classification maintained model performance and, in some cases, even improved it, while also modifying the feature space towards a desired topology. With AEs, the use of L_H slightly reduced classification performance but notably modified the feature topology. This can be useful in dimensionality reduction

applications where feature topology is more important than a slight degradation in classification performance.

These findings suggest that L_H can be useful in scenarios where controlling feature space topology is beneficial. In particular, our experiments demonstrate its applicability in *classification* and *dimensionality reduction* tasks, where modifying the topology may aid in improving generalization or enhancing the structure of low-dimensional embeddings for e.g. visualization or data compression. Beyond these tested scenarios, L_H may also hold potential in other applications discussed in Section I, such as *generative modeling*, *bioinformatics*, *transfer learning*, and *adversarial robustness*.

However, as our experiments were conducted using simple MLPs, the effects of L_H on classification performance are not fully explored and may vary with more complex models. Potential future work includes applying L_H to all neural network layers simultaneously, testing additional distance metrics, and exploring further use cases beyond classification and AEs (e.g. those mentioned in Section I). Lastly, it is important to note that the choice of an optimal distance metric in L_H can vary notably depending on the selected features and the targeted application. For example, if data is regularly spaced on the surface of a hypersphere, it is regularly spaced in terms of cosine distance but not in terms of Chebyshev distance.

ACKNOWLEDGMENT

This work was supported in part by the Research Council of Finland (grant no. 343498) and in part by the Sigrid Jusélius Foundation. The authors would like to thank Professor Okko Räsänen for the fruitful discussions and helpful comments, and Tampere Center for Scientific Computing for the computational resources used in this study. The author Einari Vaaras would also like to thank the Finnish Foundation for Technology Promotion for the encouragement grants and the Nokia Foundation for the Nokia Scholarship.

REFERENCES

- [1] W. Wan, Y. Zhong, T. Li, and J. Chen, “Rethinking Feature Distribution for Loss Functions in Image Classification,” in *Proc. IEEE CVPR*, 2018, pp. 9117–9126.
- [2] X. Hu, L. Fuxin, D. Samaras, and C. Chen, “Topology-Preserving Deep Image Segmentation,” in *Proc. NeurIPS*, 2019, pp. 5657–5668.
- [3] R. Hadsell, S. Chopra, and Y. LeCun, “Dimensionality Reduction by Learning an Invariant Mapping,” in *Proc. IEEE CVPR*, 2006, pp. 1735–1742.
- [4] B. Rafeian, P. Hermosilla, and P.-P. Vázquez, “Improving Dimensionality Reduction Projections for Data Visualization,” *Applied Sciences*, vol. 13, no. 17, 2023.
- [5] W. Wang, *Dimensionality Reduction Task*. Springer Nature Singapore, 2024, pp. 481–505.
- [6] Y. Liang, X. Li, X. Huang, Z. Zhang, and Y. Yao, “An Automated Data Mining Framework Using Autoencoders for Feature Extraction and Dimensionality Reduction,” *arXiv preprint arXiv: 2412.02211*, 2024.
- [7] I. Goodfellow, J. Pouget-Abadie, M. Mirza, B. Xu, D. Warde-Farley, S. Ozair, A. Courville, and Y. Bengio, “Generative Adversarial Nets,” in *Proc. NeurIPS*, 2014, pp. 2672–2680.
- [8] M. Lee and J. Seok, “Controllable Generative Adversarial Network,” *IEEE Access*, vol. 7, pp. 28 158–28 169, 2019.
- [9] L. Jiang, B. Dai, W. Wu, and C. C. Loy, “Focal Frequency Loss for Image Reconstruction and Synthesis,” in *Proc. IEEE ICCV*, 2021, pp. 13 919–13 929.

- [10] T. Liang, "How Well Generative Adversarial Networks Learn Distributions," *Journal of Machine Learning Research*, vol. 22, no. 228, pp. 10 366–10 406, 2021.
- [11] D. Ofer and M. Linal, "ProFET: Feature engineering captures high-level protein functions," *Bioinformatics*, vol. 31, no. 21, pp. 3429–3436, 2015.
- [12] M. Oudah and A. Henschel, "Taxonomy-aware feature engineering for microbiome classification," *BMC Bioinformatics*, vol. 19, no. 227, 2018.
- [13] K. Feuz and D. Cook, "Transfer Learning across Feature-Rich Heterogeneous Feature Spaces via Feature-Space Remapping (FSR)," *ACM Transactions on Intelligent Systems and Technology*, vol. 6, no. 1, pp. 1–27, 2015.
- [14] K. Weiss and T. Khoshgoftaar, "Evaluation of Transfer Learning Algorithms using Different Base Learners," in *Proc. IEEE ICTAI*, 2017, pp. 187–196.
- [15] S. Roy, A. Siarohin, E. Sanginetto, S. R. Bulo, N. Sebe, and E. Ricci, "Un-supervised Domain Adaptation using Feature-Whitening and Consensus Loss," in *Proc. IEEE CVPR*, 2019, pp. 9471–9480.
- [16] S. Khan, P. Yin, Y. Guo, M. Asim, and A. A. A. El-Latif, "Transfer Learning across Feature-Rich Heterogeneous Feature Spaces via Feature-Space Remapping (FSR)," *Multimedia Tools and Applications*, vol. 83, pp. 69 759–69 795, 2024.
- [17] R. Brüel-Gabrielsson, B. Nelson, A. Dwaraknath, and P. Skraba, "A Topology Layer for Machine Learning," in *Proc. AISTATS*, 2020, pp. 1553–1563.
- [18] Z. Cheng, F. Zhu, X.-Y. Zhang, and C.-L. Liu, "Delving into Feature Space: Improving Adversarial Robustness by Feature Spectral Regularization," in *Proc. ICPR*, 2024, pp. 423–439.
- [19] S. He, J. Zhuang, D. Wang, L. Peng, and J. Song, "Enhancing the Resilience of Graph Neural Networks to Topological Perturbations in Sparse Graphs," *arXiv preprint arXiv: 2406.03097*, 2024.
- [20] B. Hopkins and J. Skellam, "A New Method for determining the Type of Distribution of Plant Individuals," *Annals of Botany*, vol. 18, no. 2, pp. 213–227, 1954.
- [21] R. Lawson and P. Jurs, "New index for clustering tendency and its application to chemical problems," *Journal of Chemical Information & Computer Sciences*, vol. 30, no. 1, pp. 36–41, 1990.
- [22] G. Cross and A. Jain, "Measurement of Clustering Tendency," *IFAC Proceedings Volumes*, vol. 15, no. 1, pp. 315–320, 1982.
- [23] A. Banerjee and R. Davé, "Validating clusters using the Hopkins statistic," in *Proc. IEEE FUZZ*, 2004, pp. 149–153.
- [24] Z. Li, Z. Tian, M. Zhou, Z. Zhang, and Y. Jin, "Awareness of Line-of-Sight Propagation for Indoor Localization Using Hopkins Statistic," *IEEE Sensors Journal*, vol. 18, no. 9, pp. 3864–3874, 2018.
- [25] R. Zhang, Z. Miao, Y. Tian, and H. Wang, "A novel density peaks clustering algorithm based on Hopkins statistic," *Expert Systems with Applications*, vol. 201, p. 116892, 2022.
- [26] A. Malyugina, N. Anantrasirichai, and D. Bull, "A topological loss function for image Denoising on a new BVI-lowlight dataset," *Signal Processing*, vol. 211, no. 109081, 2023.
- [27] G. S. Alberti, J. Hertrich, M. Santacesaria, and S. Sciutto, "Manifold Learning by Mixture Models of VAEs for Inverse Problems," *Journal of Machine Learning Research*, vol. 25, no. 202, pp. 1–35, 2024.
- [28] X. Mi, F. Tang, Y. Weng, D. Wang, J. Cao, S. Tang, P. Li, and Y. Liu, "Topology-preserving Adversarial Training for Alleviating Natural Accuracy Degradation," in *Proc. BMVC*, 2024.
- [29] B. D. Ripley, "Modelling Spatial Patterns," *Journal of the Royal Statistical Society. Series B (Methodological)*, vol. 39, no. 2, pp. 172–212, 1977.
- [30] R. Dubes and A. Jain, "Clustering techniques: The user's dilemma," *Pattern Recognition*, vol. 8, no. 4, pp. 247–260, 1976.
- [31] S. Livingstone and F. Russo, "The Ryerson Audio-Visual Database of Emotional Speech and Song (RAVDESS): A dynamic, multimodal set of facial and vocal expressions in North American English," *PLoS ONE*, vol. 13, no. 5, pp. 1–35, 2018.
- [32] F. Eyben, K. Scherer, B. Schuller, J. Sundberg, E. André, C. Busso, L. Devillers, J. Epps, P. Laukka, S. Narayanan, and K. Truong, "The Geneva Minimalistic Acoustic Parameter Set (GeMAPS) for Voice Research and Affective Computing," *IEEE Transactions on Affective Computing*, vol. 7, no. 2, pp. 190–202, 2016.
- [33] F. Eyben, F. Weninger, F. Gross, and B. Schuller, "Recent developments in openSMILE, the Munich open-source multimedia feature extractor," in *Proc. ACM*, 2013, pp. 835–838.
- [34] A. Maas, R. Daly, P. Pham, D. Huang, A. Ng, and C. Potts, "Learning Word Vectors for Sentiment Analysis," in *Proc. ACL*, 2011, pp. 142–150.
- [35] J. Devlin, M. Chang, K. Lee, and K. Toutanova, "BERT: Pre-training of Deep Bidirectional Transformers for Language Understanding," in *Proc. NAACL-HLT*, 2019, pp. 4171–4186.
- [36] T. Wolf, L. Debut, V. Sanh, J. Chaumond, C. Delangue, A. Moi, P. Cistac, T. Rault, R. Louf, M. Funtowicz, J. Davison, S. Shleifer, P. von Platen, C. Ma, Y. Jernite, J. Plu, C. Xu, T. L. Scao, S. Gugger, M. Drame, Q. Lhoest, and A. M. Rush, "Transformers: State-of-the-Art Natural Language Processing," in *Proc. EMNLP*, 2020, pp. 38–45.
- [37] H. Xiao, K. Rasul, and R. Vollgraf, "Fashion-MNIST: a Novel Image Dataset for Benchmarking Machine Learning Algorithms," *arXiv preprint arXiv: 1708.07747*, 2017.
- [38] D. Hendrycks and K. Gimpel, "Gaussian Error Linear Units (GELUs)," *arXiv preprint arXiv: 1606.08415*, 2016.
- [39] D. Kingma and J. Ba, "Adam: A Method for Stochastic Optimization," in *Proc. ICLR*, 2015.
- [40] H. Mann and D. Whitney, "On a Test of Whether one of Two Random Variables is Stochastically Larger than the Other," *The Annals of Mathematical Statistics*, vol. 18, no. 1, pp. 50–60, 1947.